Proportional-integral control of propagating wave segments in excitable media

Proportional-integral control of propagating wave segments in excitable media

Hisatoshi Katsumata, Keiji Konishi,* and Naoyuki Hara
Department of Electrical and Information Systems, Osaka Prefecture University 1-1 Gakuen-cho, Naka-ku, Sakai, Osaka 599-8531 Japan
(Received 23 December 2016; published 25 April 2017)

Numerical simulations are performed to demonstrate that proportional-integral control, one of the most commonly used feedback schemes in control engineering, can stabilize propagating wave segments in excitable media to a desired size. The proportional-integral controller measures the size of a wave segment and applies a spatially uniform signal to the medium. This controller has the following features: difficult trial-and-error adjustment is not necessary, wave segments can be stabilized to different sizes without readjusting the controller, and the wave segment size can be maintained even in media having position-dependent parameters.

DOI: 10.1103/PhysRevE.95.042216

I. INTRODUCTION

Spirals, turbulence, and propagation waves in excitable media have attracted growing interest in the field of nonlinear science. Spirals and turbulence have been investigated as a cause of cardiac arrhythmias [1,2], and propagating waves are expected to be useful in engineering applications such as finding optimal paths [3], chemical logic gates [4–8], chemical memories [9,10], or information-processing devices [11–13]. As such, the control of these nonlinear phenomena has attracted considerable attention. A variety of methods for controlling excitable media have been proposed. These methods can be roughly categorized into two types: methods that eliminate nonlinear phenomena and methods that control waves or patterns.

Several methods have been proposed for eliminating nonlinear phenomena, including global nonfeedback control [14–18], local nonfeedback control [19–32], global feedback control [33–35], and local feedback control [36]. Moreover, numerous studies have shown theoretically and experimentally that waves and patterns can be controlled [37,38]. Mihaliuk *et al.* proposed a proportional feedback control method for stabilizing a segment propagating through a photosensitive Belousov-Zhabotinsky (BZ) chemical reaction system by adjusting the light intensity [39]. This proportional (P) controller applies a *position-independent* (i.e., spatially uniform) output signal to a medium by sensing the wave area in real time. Zykov *et al.* analytically investigated in detail the shape and velocity of a propagating wave stabilized by a *position-independent* proportional feedback [40–42]. Sakurai *et al.* showed that the stabilized wave can be made to propagate along a desired path by using a *position-dependent* control in combination with the *position-independent* proportional control law [43]. Steele *et al.* demonstrated that a single wave and multiple waves can be stabilized using a proportional-integral-derivative (PID) *position-independent* feedback control [44,45]. In addition, they showed that a *position-dependent* control, based on the concept of the potential function, applied in conjunction with the position-independent control enables the manipulation of propagating waves [44,45].

These studies allows us to realize that a key factor in controlling propagating unstable waves is their stabilization using *position-independent* P control. Although fundamental knowledge of such stabilization has been reported in these previous studies, for the practical situation in which excitable media have uncertain parameters, the following serious problem is inevitable: the *position-independent* P control cannot explicitly specify a desired size of propagating waves. This is because the size of the stabilized waves depends not only on the controller parameters but also on the uncertain parameters of the medium. In particular, it is difficult to design the offset in the P control law without using accurate parameters of the medium. This problem causes the following inconveniences: (1) Trial-and-error adjustment of the offset is needed in order to stabilize wave segments of a desired size; (2) even if this adjustment is successful, this controller cannot support other desired sizes unless the adjustment is performed again; and (3) the adjustment for a desired size cannot be used if the parameters of the medium are changed. These inconveniences hinder future innovative applications of excitable media.

In the present paper, we attempt to apply control theory to the above-mentioned problem. Control theory indicates that proportional-integral (PI) control, one of most popular feedback schemes in control engineering [46], has a strong potential to solve this problem because the offset is automatically adjusted for a desired size without detailed information about the medium.[1] Numerical simulations are performed in order to demonstrate that PI control can eliminate the above-mentioned inconveniences. Specifically, (1) the stabilization of a wave segment of a desired size can be automatically achieved without trial-and-error adjustment, (2) wave segments of different desired sizes can be stabilized without readjusting the controller, and (3) the desired size can be maintained even if the parameters of the medium are changed. Furthermore, we describe analytically why PI control can solve this problem while P control cannot. The present paper is a substantially extended version of our conference paper [47].

*http://www.eis.osakafu-u.ac.jp/∼ecs

[1]Although proportional-integral-derivative (PID) control, which was used for the stabilization of wave segments in previous studies [44,45], can be used to solve the above-described problem, to our knowledge, there have been few efforts to use PID control for the problem.

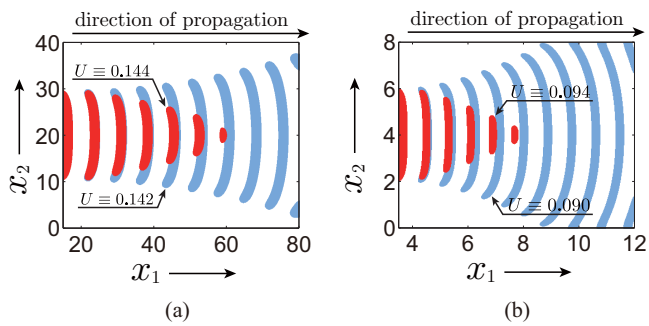

FIG. 1. Snapshots of propagating wave segments [i.e., excited area $\Omega(t)$] in the Bär model and the Oregonator model without feedback control: (a) $U \equiv 0.142$ (light-colored segments) and 0.144 (dark-colored segments) for the Bär model with $L_1 = 80$ and $L_2 = 40$, (b) $U \equiv 0.090$ (light-colored segments) and 0.094 (dark-colored segments) for the Oregonator model with $L_1 = 12$ and $L_2 = 8$. Snapshots were taken for increment of (a) $t = 4$ and (b) $t = 0.5$.

II. EXCITABLE MEDIA

In this section, we review the dynamics of excitable media without feedback control. Let us consider an excitable medium:

$$\Sigma : \begin{cases} \dfrac{\partial u}{\partial t} = F(u,v,U) + D\nabla^2 u \\ \dfrac{\partial v}{\partial t} = G(u,v,U) \end{cases} . \tag{1}$$

Here $u := u(t,\boldsymbol{x}) \in \mathbb{R}$ and $v := v(t,\boldsymbol{x}) \in \mathbb{R}$ are, respectively, the activator and inhibitor variables at position $\boldsymbol{x} := (x_1,x_2) \in [0,L_1] \times [0,L_2]$ and at time $t \in \mathbb{R}$, where $L_{1,2} > 0$ denotes the size of the medium. Moreover, $U := U(t) \in \mathbb{R}$ is the spatially uniform input signal, which does not depend on position $\boldsymbol{x}$. The nonlinear functions $F,G : \mathbb{R} \times \mathbb{R} \times \mathbb{R} \to \mathbb{R}$ describe the dynamics of reactors. $D \geqslant 0$ represents the diffusive coefficient, and $\nabla^2 := \partial^2/\partial x_1^2 + \partial^2/\partial x_2^2$ denotes the Laplacian operator. We define the excited area:

$$\Omega(t) := \{\boldsymbol{x} \in [0,L_1] \times [0,L_2] : u(t,\boldsymbol{x}) > \bar{u}\},\ t > 0, \tag{2}$$

where $\bar{u} \in \mathbb{R}$ is the threshold.

Throughout this paper, the two famous models, the Bär model [48] and the Oregonator model [49,50], are used as excitable media Σ to be controlled. The nonlinear functions of the reaction term in each model are described in Appendix A. We numerically investigate the influence of input signal U without feedback control on the excited area $\Omega(t)$ (see Appendix B for details on the numerical setup). The initial condition is provided such that the segment wave propagates in the x_1 direction. The propagating wave segments in the Bär model with constant input signals, $U \equiv 0.142$ and $U \equiv 0.144$, are shown in Fig. 1(a). The initial segment, as explained in Appendix B, expands and propagates from left to right for $U \equiv 0.142$ (light-colored segments), but disappears for $U \equiv 0.144$ (dark-colored segments). Similar behavior is observed for the Oregonator model, as shown in Fig. 1(b). These results suggest that it is difficult for a constant signal without feedback to maintain the size of the propagating segments.

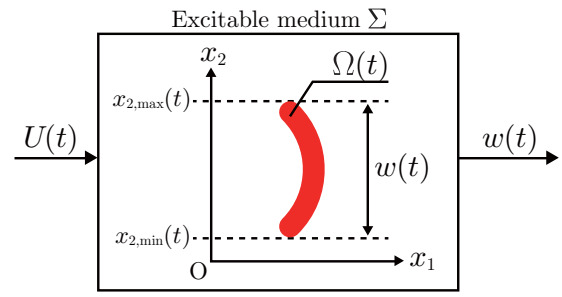

FIG. 2. Controlled object with input $U(t)$ and output $w(t)$.

III. FEEDBACK CONTROL OF EXCITABLE MEDIA

Most previous studies use P control to stabilize the propagating wave segments. In this section, P control is reviewed, and its drawback with respect to numerical simulation is discussed. In order to overcome this drawback, we use PI control, which is well known in control theory. An analysis is performed in order to demonstrate why PI control works well.

A. Proportional control

As shown in Fig. 2, the excitable medium Σ is treated as a controlled object with input signal $U(t)$ and output signal $w(t) \in \mathbb{R}$. The output signal, $w(t)$, which is the width of the propagating wave segment, is defined as follows:

$$w(t) := x_{2,\max}(t) - x_{2,\min}(t),$$
$$x_{2,\max}(t) := \max_{\boldsymbol{x} \in \Omega(t)} x_2,\ x_{2,\min}(t) := \min_{\boldsymbol{x} \in \Omega(t)} x_2.$$

As shown in Fig. 3, this object is controlled by the input signal:

$$U(t) = K_{\mathrm{P}} e(t) + I, \tag{3}$$

where $K_{\mathrm{P}} \in \mathbb{R}$ and $I \in \mathbb{R}$ are the proportional feedback gain and the offset, respectively. Moreover, $e(t) \in \mathbb{R}$ is the error between the width $w(t)$ and the reference signal $r(t) \in \mathbb{R}$:

$$e(t) := r(t) - w(t). \tag{4}$$

The reference signal $r(t)$, which is the desired width of the propagating wave segments, is given by the user.

We evaluate the performance of the P control system through numerical simulations. Figure 4(a) shows that the P controller (3) with the control parameters $K_{\mathrm{P}} = -3 \times 10^{-3}$, $I = 0.15$, and desired width $r(t) \equiv 20$ successfully stabilizes a propagating wave segment in the Bär model (A1). However, the width of the segment, $w(t)$, does not converge to the desired width $r(t) \equiv 20$, and the error $e(t)$ does not become zero. Similar results were obtained for the Oregonator model (A2) with $K_{\mathrm{P}} = -3 \times 10^{-3}$, $I = 0.093$, and $r(t) \equiv 4$, as shown in Fig. 4(b).

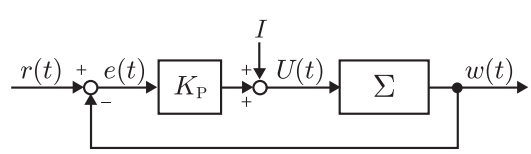

FIG. 3. Block diagram of the feedback control system consisting of excitable medium Σ and the P controller (3).

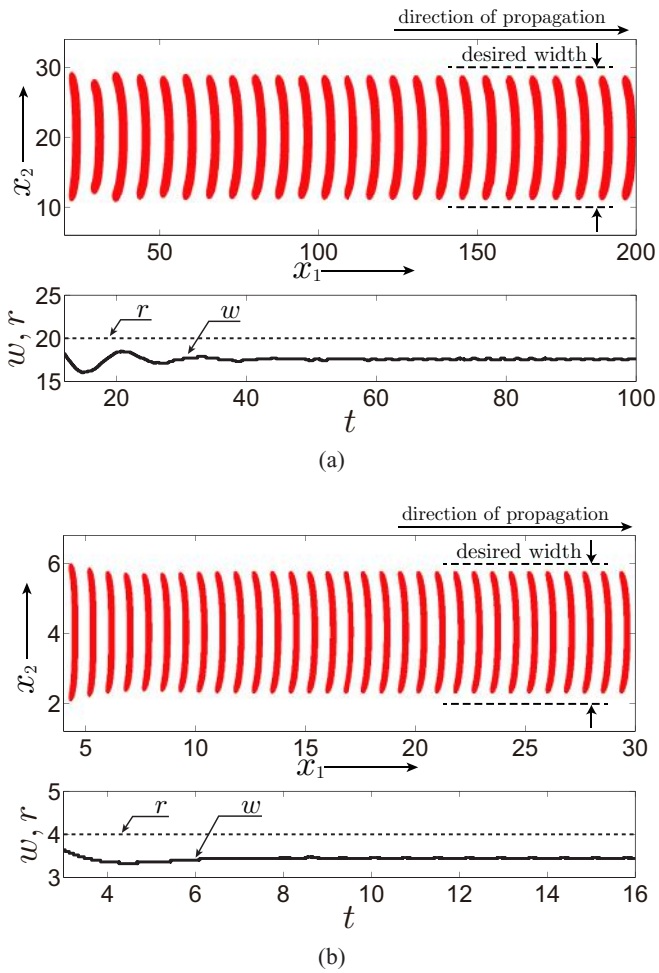

FIG. 4. Snapshots and time series data of propagating wave segments with P control in (a) the Bär model ($L_1 = 200$ and $L_2 = 40$) and (b) the Oregonator model ($L_1 = 30$ and $L_2 = 8$). (a) Bär model with $K_\mathrm{P} = -3 \times 10^{-3}$, $I = 0.15$, and $r(t) \equiv 20$. (b) Oregonator model with $K_\mathrm{P} = -3 \times 10^{-3}$, $I = 0.093$, and $r(t) \equiv 4$.

Note that the error $e(t)$ can be zero if a suitable offset I is known. However, since the offset strongly depends on the model parameters, it is generally not easy to find a suitable offset in advance. As a result, in practical situations, we usually do not stabilize the segment to the desired width. This drawback is well known in the field of control theory [46]. In order to overcome this drawback, control theory recommends the use of PI control. In the next section, PI control will be used in order to eliminate the error.

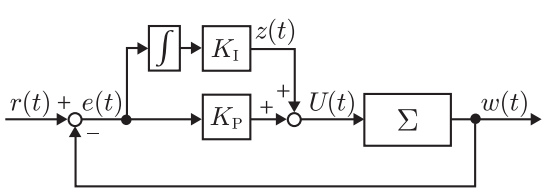

FIG. 5. Block diagram of the feedback control system consisting of excitable medium Σ and PI controller (5).

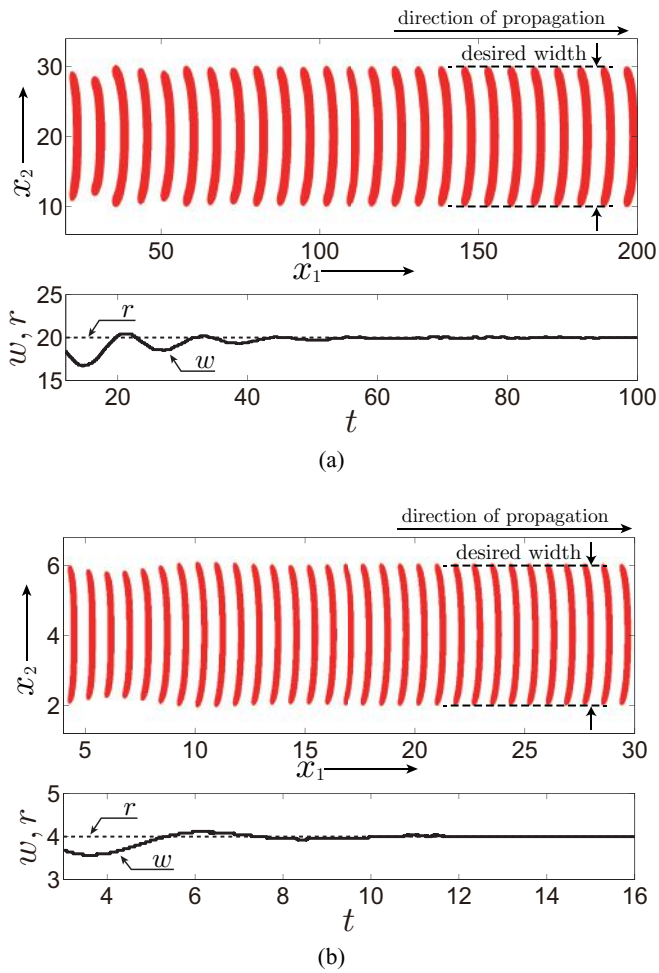

FIG. 6. Snapshots and time series data of propagating wave segments with PI control in (a) the Bär model ($L_1 = 200$ and $L_2 = 40$) and (b) the Oregonator model ($L_1 = 30$ and $L_2 = 8$). (a) Bär model with $K_\mathrm{P} = -3 \times 10^{-3}$, $K_\mathrm{I} = -2 \times 10^{-4}$, $r(t) \equiv 20$, and $z(0) = 0.15$. (b) Oregonator model with $K_\mathrm{P} = -3 \times 10^{-3}$, $K_\mathrm{I} = -2 \times 10^{-3}$, $r(t) \equiv 4$, and $z(0) = 0.093$.

B. Proportional-integral control

The control law for the PI controller is given by

$$\begin{cases} U(t) &= K_\mathrm{P} e(t) + z(t) \\ \dfrac{dz(t)}{dt} &= K_\mathrm{I} e(t) \end{cases}, \tag{5}$$

where $K_\mathrm{P} \in \mathbb{R}$ and $K_\mathrm{I} \in \mathbb{R}$ are the feedback gains, $z(t) \in \mathbb{R}$ is the additional state variable of PI controller (5). The feedback control system consisting of excitable medium Σ and PI controller (5) is shown in Fig. 5.

We confirm the performance of the PI control system through numerical simulations. The snapshots and time series data of propagating wave segments with PI control (5) in the Bär model (A1) are shown in Fig. 6(a). The PI controller (5) with $K_\mathrm{P} = -3 \times 10^{-3}$ and $K_\mathrm{I} = -2 \times 10^{-4}$ successfully stabilizes the propagating wave segment to the desired width $r(t) \equiv 20$ without steady-state error. Similar results were obtained for the Oregonator model (A2), as shown in Fig. 6(b).

The numerical results indicate that PI control can solve the problem of P control.

C. Analytical approach

The previous subsections showed numerically that P control causes the steady state error, but PI control does not. In this subsection, we analytically demonstrate the reason for this.

As it stands now, we cannot analytically extract the detailed mathematical model of the controlled object illustrated in Fig. 2 from excitable medium Σ. On the other hand, Sakurai and Osaki showed that the dynamics of a propagating wave segment in the Oregonator model can be reduced to that of a two-dimensional ordinary differential equation having an unstable equilibrium point [51]. This equilibrium point corresponds to an unstable propagating wave segment. Based on this reduction, let us assume that the dynamics around the unstable equilibrium point (i.e., the unstable segment), with a desired constant width $r(t) \equiv w_0$ and the suitable offset $I = U_0$, can be roughly described by a linear system:

$$\begin{cases} \dfrac{\mathrm{d}\mathbf{x}(t)}{\mathrm{d}t} &= \boldsymbol{A}\mathbf{x}(t) + \boldsymbol{b}\Delta U(t) \\ \Delta w(t) &= \boldsymbol{c}\mathbf{x}(t) \end{cases}, \tag{6}$$

where $\Delta U(t) := U(t) - U_0$ and $\Delta w(t) := w(t) - w_0$. Here $\mathbf{x}(t) \in \mathbb{R}^n$ is the state variable. Moreover, $\boldsymbol{A} \in \mathbb{R}^{n\times n}$, $\boldsymbol{b} \in \mathbb{R}^n$, and $\boldsymbol{c} \in \mathbb{R}^{1\times n}$ are the system matrices.

For P control, the closed-loop system consisting of controlled object (6) and P controller (3) around the unstable equilibrium point is described by

$$\frac{d\mathbf{x}(t)}{dt} = (\boldsymbol{A} - K_{\mathrm{P}}\boldsymbol{b}\boldsymbol{c})\mathbf{x}(t) + \boldsymbol{b}(K_{\mathrm{P}}\Delta\bar{r} + \Delta I), \tag{7}$$

where $\Delta\bar{r} := \bar{r} - w_0$ and $\Delta I := I - U_0$. Here $\bar{r}$ is the constant reference signal. If K_{P} is designed such that $\boldsymbol{A} - K_{\mathrm{P}}\boldsymbol{b}\boldsymbol{c}$ is stable, then closed-loop system (7) converges to the stable equilibrium point:

$$\mathbf{x}^* = -(\boldsymbol{A} - K_{\mathrm{P}}\boldsymbol{b}\boldsymbol{c})^{-1}\boldsymbol{b}(K_{\mathrm{P}}\Delta\bar{r} + \Delta I). \tag{8}$$

As a result, the output signal $w(t)$ converges to $\bar{r}$, which indicates that $\Delta w^* := \boldsymbol{c}\mathbf{x}^* = \Delta\bar{r}$ holds only if I is set to

$$I = -\Delta\bar{r}\left\{\frac{1}{\boldsymbol{c}(\boldsymbol{A} - K_{\mathrm{P}}\boldsymbol{b}\boldsymbol{c})^{-1}\boldsymbol{b}} + K_{\mathrm{P}}\right\} + U_0, \tag{9}$$

which depends on the system matrices $(\boldsymbol{A},\boldsymbol{b},\boldsymbol{c})$ and the suitable offset U_0. Note that, in practical situations, it is difficult to obtain these matrices and the offset precisely in advance. Therefore, steady-state error $\lim_{t\to\infty}\{\bar{r} - w(t)\} = \Delta\bar{r} - \Delta w^*$ inevitably occurs.

For PI control, controlled object (6) and PI controller (5) around the unstable equilibrium point provide the following closed-loop system:

$$\frac{d}{dt}\begin{bmatrix}\mathbf{x}(t)\\ \Delta z(t)\end{bmatrix} = \begin{bmatrix}(\boldsymbol{A} - K_{\mathrm{P}}\boldsymbol{b}\boldsymbol{c}) & \boldsymbol{b}\\ -K_{\mathrm{I}}\boldsymbol{c} & 0\end{bmatrix}\begin{bmatrix}\mathbf{x}(t)\\ \Delta z(t)\end{bmatrix} + \begin{bmatrix}\boldsymbol{b}K_{\mathrm{P}}\\ K_{\mathrm{I}}\end{bmatrix}\Delta\bar{r}, \tag{10}$$

where $\Delta z(t) := z(t) - U_0$. If K_{P} and K_{I} are designed such that closed-loop system (10) is stable, then its trajectories converge on stable equilibrium point $[\mathbf{x}^{*T}\ \Delta z^*]^T$ satisfying

$$\begin{bmatrix}\mathbf{0}\\ 0\end{bmatrix} = \begin{bmatrix}(\boldsymbol{A} - K_{\mathrm{P}}\boldsymbol{b}\boldsymbol{c}) & \boldsymbol{b}\\ -K_{\mathrm{I}}\boldsymbol{c} & 0\end{bmatrix}\begin{bmatrix}\mathbf{x}^*\\ \Delta z^*\end{bmatrix} + \begin{bmatrix}\boldsymbol{b}K_{\mathrm{P}}\\ K_{\mathrm{I}}\end{bmatrix}\Delta\bar{r}. \tag{11}$$

The second row of this equation indicates that

$$\Delta w^* = \boldsymbol{c}\mathbf{x}^* = \Delta\bar{r}. \tag{12}$$

Consequently, we have no steady-state error: $\lim_{t\to\infty}\{\bar{r} - w(t)\} = \Delta\bar{r} - \Delta w^* = 0$. Note that the error becomes zero as long as closed-loop system (10) is stable.

The arguments of the steady-state error mentioned above provide a legitimate reason why P control has steady-state error but PI control does not. These arguments are well known in control theory [46].

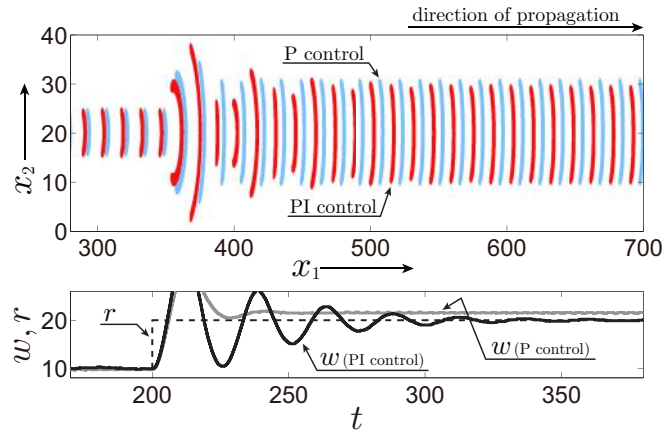

FIG. 7. Snapshots and time series data of propagating wave segments with P and PI control in the Bär model ($L_1 = 700$ and $L_2 = 40$) for the size change: $r(t) \equiv w_0 = 10$ to $r(t) \equiv \bar{r} = 20$ at $t = 200$. P control with $K_{\mathrm{P}} = -1 \times 10^{-3}$ and $I = U_0 = 0.1413$ and PI control with $K_{\mathrm{P}} = -1 \times 10^{-3}$, $K_{\mathrm{I}} = -1 \times 10^{-4}$, and $z(0) = 0.14$. Snapshots were taken every $t = 8$.

IV. NUMERICAL SIMULATIONS

The preceding section showed numerically and analytically that PI control can solve the serious problem of P control, which causes the three inconveniences mentioned earlier. As shown in Fig. 6, the need for trial-error adjustment of the offset I was eliminated owing to the automatic adjustment mechanism of PI control. In this section, we demonstrate through numerical simulations that PI control can eliminate the second and third inconveniences.

We consider the second inconvenience. Namely, even though the offset $I = U_0$ of P control is successfully decided for a desired size w_0 [see Eq. (9)], steady-state error occurs for other desired sizes. Figure 7 shows snapshots and time series data of propagating wave segments with P and PI control in the Bär model (A1). P control with the ideal offset $I = U_0 = 0.1413$ for a desired size $r(t) \equiv w_0 = 10$ does not induce steady-state error until $t = 200$. The size is changed to $r(t) \equiv \bar{r} = 20$ at $t = 200$, and then a small error occurs due to the nonideal offset. In contrast, PI control does not induce steady-state error for both sizes owing to the automatic adjustment mechanism. These results indicate that PI control can eliminate the second inconvenience.

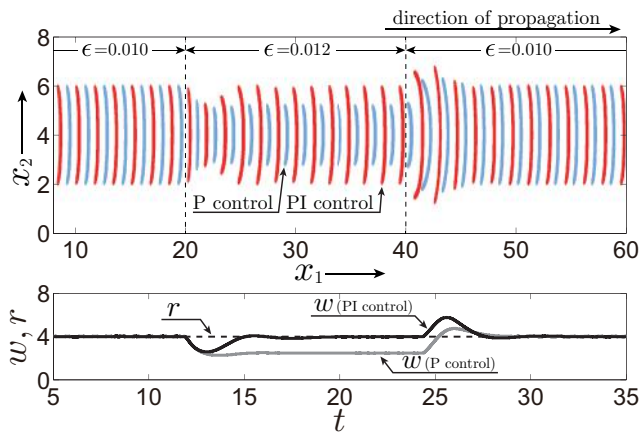

FIG. 8. Snapshots and time series data of propagating wave segments with P and PI control in the Oregonator model ($L_1 = 60$ and $L_2 = 8$), the parameter ε of which depends on position: $\varepsilon = 0.010$ in $x_1 \in [0,20] \cup [40,60]$ and $\varepsilon = 0.012$ in $x_1 \in (20,40)$. P control with $K_\mathrm{P} = -4 \times 10^{-3}$ and $I = U_0 = 0.0913$ and PI control with $K_\mathrm{P} = -4 \times 10^{-3}$, $K_\mathrm{I} = -2 \times 10^{-3}$, and $z(0) = 0.091$. Snapshots were taken every $t = 1$.

As described previously, the third inconvenience is that P control with the ideal offset $I = U_0$ for a desired size $r(t) \equiv w_0$ cannot maintain the size if media parameters are changed. Snapshots and time series data of propagating wave segments with P and PI control in the Oregonator model (A2) are shown in Fig. 8. Let us consider the realistic situation in which the media parameters depend on position $\boldsymbol{x}$. Here, the parameter ε depends on position as follows: $\varepsilon = 0.010$ in $x_1 \in [0,20] \cup [40,60]$ and $\varepsilon = 0.012$ in $x_1 \in (20,40)$. P control with the ideal offset $I = U_0 = 0.0913$ for desired size $r(t) \equiv w_0 = 4$ on $\varepsilon = 0.010$ does not induce steady-state error in $x_1 \in [0,20]$, but does induce a large error in $x_1 \in (20,40)$ due to the nonideal offset. On the other hand, PI control does not induce steady-state error for any position. Thus, it is numerically verified that the third inconvenience can be eliminated by PI control.

The analytical and numerical results mentioned above suggest that the adjustment of offset I for P control is fragile for the case with no steady-state error, because I should be set to a unique point described by Eq. (9). In contrast, the design of K_P and K_I for PI control is robust, because these parameters only have to be designed such that closed system (10) becomes stable. In order to confirm the robustness of the design, we conduct numerical simulations for a variety of K_P and K_I, as shown in Fig. 9. The open circles (crosses) indicate the set $(K_\mathrm{P}, K_\mathrm{I})$ for which the steady-state error converges (does not converge) to zero (see Appendix C for details). Snapshots and time series data of propagating wave segments at the filled circles are shown in Fig. 6. For both the Bär model [Fig. 9(a)] and the Oregonator model [Fig. 9(b)], stabilization without steady-state error can be achieved for large region of the K_P-K_I space.

V. CONCLUSIONS

We have demonstrated that PI control can stabilize propagating wave segments to a desired size without steady-state error. Numerical simulations have demonstrated that PI control has the following advantages: there is no need to conduct difficult trial-and-error adjustment in order to achieve the no-steady-state-error condition, the size of the wave segment can be varied without readjustment of control, and the desired size can be obtained even for the situation in which the media parameters are position dependent.

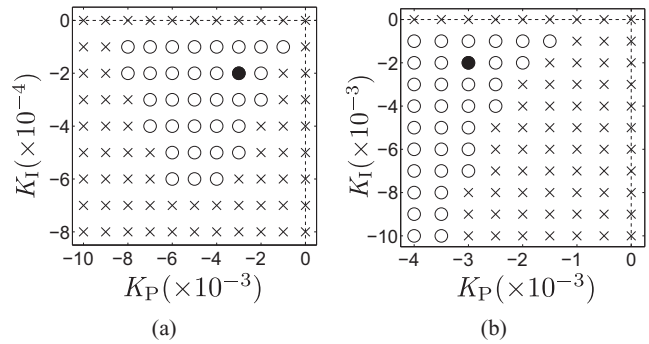

FIG. 9. Stability regions on K_P-K_I space for (a) the Bär model ($L_1 = 300$ and $L_2 = 40$) and (b) the Oregonator model ($L_1 = 40$ and $L_2 = 8$). Open circles indicate that stabilization without steady-state error is achieved, whereas crosses indicate that stabilization without steady-state error is not achieved.

Although PI control overcomes the serious problem of P control, we noticed through numerical simulations that the proposed control system is vulnerable to the initial conditions and external disturbances. This suggests that the proposed control system requires further development but also implies that robust control theory concepts can be applied to excitable media. The key to developing the proposed control system based on these concepts is to identify system (6). If system (6) is experimentally identified, it is expected that a number of schemes developed for control theory can be directly applied to excitable media in order to improve the control performance.

ACKNOWLEDGMENT

The present study was supported in part by JSPS KAKENHI (Japan), 26289131.

APPENDIX A: BÄR MODEL AND OREGONATOR MODEL

The reaction term of the Bär model [48] with the input signal U is described by

$$\begin{aligned} F(u,v,U) &:= \frac{1}{\epsilon}u(1-u)\left(u - \frac{v+b}{a}\right), \\ G(u,v,U) &:= g(u) - v + U, \\ g(u) &:= \begin{cases} 0 & u < 1/3 \\ 1 - 6.75u(u-1)^2 & 1/3 \leqslant u \leqslant 1 \\ 1 & u > 1 \end{cases}, \end{aligned} \tag{A1}$$

where the parameters are fixed as $\epsilon = 0.03$, $a = 0.84$, $b = 0.07$, and $D = 1.0$. The Oregonator model with input signal U [49,50] has the reaction term:

$$\begin{aligned} F(u,v,U) &:= \frac{1}{\epsilon}\left[u - u^2 - (av+U)\frac{u-b}{u+b}\right], \\ G(u,v,U) &:= u - v, \end{aligned} \tag{A2}$$

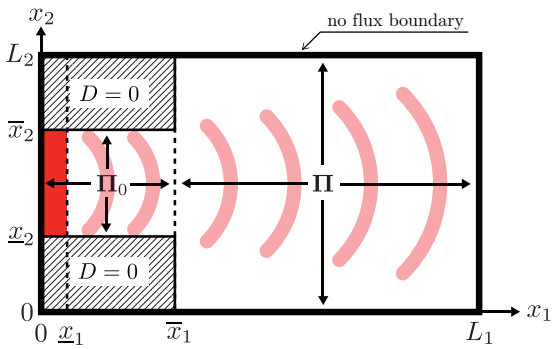

FIG. 10. Schematic diagram of an excitable medium consisting of region $\mathbf{\Pi}_0$ without feedback control and region $\mathbf{\Pi}$ with feedback control for the numerical simulations of the present study.

with the parameters $\epsilon = 0.01$, $a = 2.5$, $b = 0.002$, and $D = 0.1$.

APPENDIX B: SETUP FOR THE NUMERICAL SIMULATIONS

The numerical simulations of the present study were performed using the explicit Euler method with time step $\Delta t = 2 \times 10^{-3}$ and grid size $\Delta x = 0.1$ for the Bär model and with time step $\Delta t = 2 \times 10^{-4}$ and grid size $\Delta x = 0.02$ for the Oregonator model. Both models have no-flux boundary. The threshold $\bar{u}$ used in Eq. (2) is set to $\bar{u} = b/a$ for the Bär model and $\bar{u} = 0.1$ for the Oregonator model.

The initial condition is set up based on findings reported in a previous study [52]. Figure 10 shows the excitable media used in the numerical simulations of the present study. In the region $\mathbf{\Pi}_0$ between the two no-diffusion ($D = 0$) areas (i.e., shaded areas), an initial propagating segment with constant input signal $U(t) \equiv \hat{U}$ is generated by the initial state:

$$\begin{bmatrix} u(0,\boldsymbol{x}) \\ v(0,\boldsymbol{x}) \end{bmatrix} = \begin{cases} \begin{bmatrix} 0.5 & 0 \end{bmatrix}^T & \boldsymbol{x} \in \left[0,\underline{x}_1\right] \times \left[\underline{x}_2,\overline{x}_2\right] \\ \begin{bmatrix} 0 & 0 \end{bmatrix}^T & \text{otherwise} \end{cases}.$$

The propagating segment moves out of region $\mathbf{\Pi}_0$ and into controlled region $\mathbf{\Pi}$, where the spatially uniform input signal $U(t)$ is added as follows: constant input signals for Fig. 1 and P control (3) and PI control (5) for Figs. 4 through 8. The parameters for these setups are as follows: $\hat{U} = 0.14$, $\underline{x}_1 = 1$, $\overline{x}_1 = 20$, $\underline{x}_2 = 10$, and $\overline{x}_2 = 30$ for the Bär model; and $\hat{U} = 0.09$, $\underline{x}_1 = 0.2$, $\overline{x}_1 = 4$, $\underline{x}_2 = 2$, and $\overline{x}_2 = 6$ for the Oregonator model. As an exception, we use $\underline{x}_2 = 15$, and $\overline{x}_2 = 25$ for the Bär model in Fig. 7.

APPENDIX C: NUMERICAL PROCEDURE FOR FIG. 9

The numerical procedure used to check the steady-state error in Fig. 9 consists of the following four steps: (1) a gain set $(K_\mathrm{P}, K_\mathrm{I})$ is fixed; (2) numerical simulations using the feedback control system shown in Fig. 5 with the setup described in Appendix B are conducted; and (3) an open circle is plotted in Fig. 9 if $w(t)$ converges to the desired width (i.e., $|w(t) - w_0| < w_\mathrm{th}, \forall t \in [T_0, T_1]$), otherwise a cross is plotted. In order to obtain Fig. 9, this procedure was conducted for various sets $(K_\mathrm{P}, K_\mathrm{I})$. The parameters used in the procedure are as follows: $z(0) = 0.150$, $w_0 = 20$, $w_\mathrm{th} = 1.0$, $T_0 = 120$, and $T_1 = 160$ for the Bär model, and $z(0) = 0.093$, $w_0 = 4$, $w_\mathrm{th} = 0.2$, $T_0 = 16$, and $T_1 = 20$ for the Oregonator model.

[1] D. Zipes and J. Jalife, *Cardiac Electrophysiology: From Cell to Bedside* (Saunders, Philadelphia, PA, 2009).
[2] S. Sinha and S. Sridhar, *Patterns in Exitable Media: Genesis, Dynamics, and Control* (CRC Press/Taylor & Francis, Boca Raton, FL, 2015).
[3] O. Steinbock, A. Toth, and K. Showalter, Science **267**, 868 (1995).
[4] A. Adamatzky, Chaos, Solitons Fractals **21**, 1259 (2004).
[5] A. Adamatzky and B. De Lacy Costello, Chaos, Solitons Fractals **34**, 307 (2007).
[6] R. Toth, C. Stone, A. Adamatzky, B. De Lacy Costello, and L. Bull, Chaos, Solitons Fractals **41**, 1605 (2009).
[7] A. Adamatzky, Phys. Rev. E **92**, 032811 (2015).
[8] A. Adamatzky, PLoS ONE **11**, e0168267 (2016).
[9] I. Motoike and K. Yoshikawa, Phys. Rev. E **59**, 5354 (1999).
[10] I.N. Motoike, K. Yoshikawa, Y. Iguchi, and S. Nakata, Phys. Rev. E **63**, 036220 (2001).
[11] R. Toth, C. Stone, A. Adamatzky, B. De Lacy Costello, and L. Bull, J. Chem. Phys. **129**, 184708 (2008).
[12] J. Stovold and S. O'Keefe, Int. J. Parallel, Emerg. Distr. Syst. **32**, 74 (2017).
[13] A. Adamatzky, *Advances in Unconventional Computing: Prototypes, Models and Algorithms* (Springer, Cham, Switzerland, 2017).
[14] G. V. Osipov and J. J. Collins, Phys. Rev. E **60**, 54 (1999).
[15] S. Alonso, F. Sagues, and A. S. Mikhailov, Science **299**, 1722 (2003).
[16] S. Takagi, A. Pumir, D. Pazó, I. Efimov, V. Nikolski, and V. Krinsky, Phys. Rev. Lett. **93**, 058101 (2004).
[17] S. Alonso, F. Sagués, and A. S. Mikhailov, Chaos **16**, 023124 (2006).
[18] H. Sakaguchi and Y. Kido, Prog. Theor. Phys. **161**, 332 (2006).
[19] A. T. Stamp, G. V. Osipov, and J. J. Collins, Chaos **12**, 931 (2002).
[20] S. A. Vysotsky, R. V. Cheremin, and A. Loskutov, J. Phys.: Conf. Series **23**, 202 (2005).
[21] H. Sakaguchi and Y. Kido, Phys. Rev. E **71**, 052901 (2005).
[22] Z. Cao, H. Zhang, F. Xie, and G. Hu, Europhys. Lett. **75**, 875 (2006).
[23] Z. Cao, P. Li, H. Zhang, F. Xie, and G. Hu, Chaos **17**, 015107 (2007).
[24] G. Tang, M. Deng, B. Hu, and G. Hu, Phys. Rev. E **77**, 046217 (2008).
[25] J.-X. Chen, J.-W. Mao, B. Hu, J.-R. Xu, Y.-F. He, Y. Li, and X.-P. Yuan, Phys. Rev. E **79**, 066209 (2009).
[26] H. Zhang, B. Hu, and G. Hu, Phys. Rev. E **68**, 026134 (2003).
[27] Y.Q Fu, H. Zhang, Z. Cao, B. Zheng, and G. Hu, Phys. Rev. E **72**, 046206 (2005).

[28] G. Yuan, G. Wang, and S. Chen, Europhys. Lett. **72**, 908 (2005).
[29] H. Zhang, Z. Cao, N.-J. Wu, H.-P. Ying, and G. Hu, Phys. Rev. Lett. **94**, 188301 (2005).
[30] A. Y. Loskutov and S. A. Vysotskii, JETP Lett. **84**, 524 (2006).
[31] S. Sinha, A. Pande, and R. Pandit, Phys. Rev. Lett. **86**, 3678 (2001).
[32] S. Sridhar and S. Sinha, Europhys. Lett. **81**, 50002 (2008).
[33] H. Sakaguchi and Y. Nakamura, J. Phys. Soc. Jpn. **79**, 074802 (2010).
[34] K. Konishi, M. Takeuchi, and T. Shimizu, Chaos **21**, 023101 (2011).
[35] M. Takeuchi, K. Konishi, and N. Hara, Cybern. Phys. **1**, 73 (2012).
[36] W. Guo, C. Qiao, Z. Zhang, Q. Ouyang, and H. Wang, Phys. Rev. E **81**, 056214 (2010).
[37] A. Mikhailov and K. Showalter, Phys. Rep. **425**, 79 (2006).
[38] K. Showalter and I. R. Epstein, Chaos **25**, 097613 (2015).
[39] E. Mihaliuk, T. Sakurai, F. Chirila, and K. Showalter, Phys. Rev. E **65**, 065602 (2002).
[40] V. S. Zykov and K. Showalter, Phys. Rev. Lett. **94**, 068302 (2005).
[41] S. V. Zykov, Eur. Phys. J. Special Topics **157**, 209 (2008).
[42] A. Kothe, V. S. Zykov, and H. Engel, Phys. Rev. Lett. **103**, 154102 (2009).
[43] T. Sakurai, E. Mihaliuk, F. Chirila, and K. Showalter, Science **296**, 2009 (2002).
[44] A. J. Steele, M. Tinsley, and K. Showalter, Chaos **18**, 026108 (2008).
[45] R. M. Tinsley, J. A. Steele, and K. Showalter, Eur. Phys. J. Special Topics **165**, 161 (2008).
[46] N. Nise, *Control Systems Engineering* (The Benjamin/Cummings, Redwood, CA, 1995).
[47] H. Katsumata, K. Konishi, and N. Hara, Proc. of SICE Annual Conference (2016), p. 898.
[48] M. Bär and M. Eiswirth, Phys. Rev. E **48**, R1635 (1993).
[49] H. J. Krug, L. Pohlmann, and L. Kuhnert, J. Phys. Chem. **94**, 4862 (1990).
[50] S. Kadar, T. Amemiya, and K. Showalter, J. Phys. Chem. A **101**, 8200 (1997).
[51] T. Sakurai and K. Osaki, Commun. Nonlinear Sci. Numer. Simul. **13**, 1067 (2008).
[52] E. Mihaliuk, T. Sakurai, F. Chirila, and K. Showalter, Faraday Discuss. **120**, 383 (2002).